Optical Flow Computation Based Medical Motion Estimation of Cardiac Ultrasound Imaging

Qishan Luo[1] and Dong C.Liu[1]

[1]School of Computer Science, Sichuan University,
Chengdu, China
Email: luoluo338@163.com

***Abstract*— OF(optical flow) Computation is widely used in image registration, motion analyzing, and motion object detection. This paper employs OF computation in estimating the motion of cardiac ultrasound imaging. The OF computation is achieved by a method called LSF(least squares formulation). In sufficiently small region of interest in the image plane and small time interval, the OF vector can be formulated as a linear least square method .Preventing the imaging is ill-conditioned, we improve the LSF method by adding the concept of regularization. Since this improving, we can greatly reduce the appearance of ill OF vector. The experiments are consisted of three groups trials: the previous two trials are based on simulation imaging, and the last one is based on real cardiac ultrasound imaging. The motion vector is finally expressed in Vector diagram. This method has better accuracy than MSAD(minimum sum of absolute difference).**

Keywords-OF; motion estimation; LSF; cardiac ultrasound imaging; regularization

I. INTRODUCTION

Ultrasound has been widely used in medical field and supplies us a powerful tool in clinical diagnosis and treatment. The cardiac ultrasound application, which acts as an important branch of ultrasound field, attracts attention from more and more scholars. In this application, motion analysis of the cardiac structure and tissue helps doctors to catch the cardiac healthy condition of sufferers. There is a category of algorithm called OF(optical flow), which is raised for motion problem. OF is a classical algorithm in motion analysis and motion object detection. Hundreds of methods has been proposed to solve the OF computation. Most of the methods are classically based on the well-known Horn and Schunck model [1].

The process of recovering OF embody a set of assumptions which, simply saying, may be violated by many factors. We have to consider lots of situation that violates the brightness constancy: the motion boundaries, shadows, or specular reflections. For the aim of reducing the possibility of assumption violation, it is necessary to denoise and smoothe the ultrasound imaging. The traditional technology based on optical flow computation costs many matrix operations and lots of time on iterating, but it's much more accurate in motion estimating comparing with the algorithms with none optical flow model, like MSAD and correlation.

When recovering the OF vector field, we employ the LSF(least squares formulation) as the OF algorithm. We make an linear decomposition to the motion vector of each pixel and bring it to the OF constraints equation. Through minimizing the sum of luminous intensity variation in the ROI, we can get the motion vector. However, when we do the SVD(singular value decomposition), there exists another problem: the image is possibly to be ill-conditioned [2]. If that case, the OF vector of the ill-conditioned area will be infinite large. Hence we have to regularize the matrix need to do SVD operation in the algorithm. Follow that step, we can avoid the motion vector ill-large. Visualization of motion vector is the ending step of this experiment. After getting the motion vector of each pixel, we will translate them into a vector diagram, which clearly express the motion pattern. In this paper, we take three groups of trials. The experiment starts with a simulation imaging trials. We compare the calculated OF vector field with the standard vector field, and get the error rate, which satisfies us. Next, we test the algorithm on a series of real continuous cardiac frames. To our joy the result is very good.

This paper is organized as follows: some basically optical flow knowledge is mentioned in Section II. The LSF algorithm is describe in Section III, the extended algorithm LSF with regularization is discussed in Section IV. The experiment and results are demonstrated in Section V, Conclusions and future work are given in Section VI.

II. ESTIMATING OPTICAL FLOW

The initial hypothesis in measuring image motion is that the intensity structures of local time-varying image regions are approximately constant under motion for at least a short duration [1]. So we have:

$$I(X,t) \approx I(X+\delta X, t+\delta t). \tag{1}$$

I(X, t) is the image intensity at time t; δx is the displacement of the local image region at (x, t) after time δt. Expanding the left-hand side of this equation in a Taylor series yields, we have the famous optical flow constraints equation:

$$\nabla I \cdot V + I_t = 0. \tag{2}$$

Where $\nabla I = (I_x, I_y)$ is the spatial intensity gradient and V = (u, v) is the image velocity. As V (u, v) has two unknown variable u and v and only one equation is known, we need other constraints to get the velocity [3]. Different methods are developed to fit to OF model. They can be classified into two main groups: local methods such as the Lucas–Kanade technique and global methods such as the Horn/Schunck approach [4]. Often local methods are more robust under noise, while global techniques yield dense flow fields [5]. In this paper, the method faces the global level. As OF method can be easily effected by the noise, we try to denoise the ultrasound image by a box filter as the first step. Then we take this denoised picture as the input of next step.

III. Least Squares Formulation for Optical Flow Computation

We formulate the optical flow computation as a linear least square method in sufficiently small region of interest in the image plane and small time interval [6]. Several basical motion patterns can be simulated in this model, like: translation, rotation, scaling. We create the following translation:

$$\begin{bmatrix} U \\ V \end{bmatrix} = \begin{bmatrix} A & B \\ C & D \end{bmatrix} \begin{bmatrix} x \\ y \end{bmatrix} + \begin{bmatrix} a \\ b \end{bmatrix} . \tag{3}$$

(U, V) stands for the velocity vector, (a, A, B, b, C, D) is the translation parameter of point (x, y). Bring (3) into the OF constraints equation, we get the new lineared constraints equation:

$$I_x a + I_x Ax + I_x By + I_y b + I_y Cx + I_y Dy + I_t = 0 . \tag{4}$$

The partial derivatives of I_x, I_y and I_t in (4) will be estimated by using the finite difference method [4]:

$$I_x \approx \frac{1}{4}[I_{i,j+1,k} - I_{i,j,k} + I_{i+1,j+1,k} - I_{i+1,j,k} + I_{i,j+1,k+1} - I_{i,j,k+1} + I_{i+1,j+1,k+1} - I_{i+1,j,k+1}] \tag{5}$$

$$I_y \approx \frac{1}{4}[I_{i+1,j,k} - I_{i,j,k} + I_{i+1,j+1,k} - I_{i,j+1,k} + I_{i+1,j,k+1} - I_{i,j,k+1} + I_{i+1,j+1,k+1} - I_{i,j+1,k+1}] \tag{6}$$

$$I_t \approx \frac{1}{4}[I_{i,j,k+1} - I_{i,j,k} + I_{i+1,j,k+1} - I_{i+1,j,k} + I_{i,j+1,k+1} - I_{i,j+1,k} + I_{i+1,j+1,k+1} - I_{i+1,j+1,k}] \tag{7}$$

For convenience, we write the parameters (a, A, B, b, C, D) as the vector $\vec{x}$,the discrete values vector $(I_x, I_x x, I_x y, I_y, I_y x, I_y y)$ as coefficient vector $\vec{a}$, and I_t as the coefficient f. Both (2) and (4) provide one error per pixel, which leads to the question of how these errors are aggregated over the image [7]. Assuming the error to be very small, so we minimize the sum of the error in the ROI. For N pixels within the ROI, (4) could be formulated as a least square method,

$$\min_{x_j} \sum_{i=1}^{N} \left(\sum_{j=1}^{6} a_j^{(i)} x_j + f^{(i)}\right)^2 = \min_{x_j} 2\left[\frac{1}{2}\vec{x}^T \sum_{i=1}^{N} A^{(i)}\vec{x} + \left(\sum_{i=1}^{N} f^{(i)} a^{(i)}\right)\cdot \vec{x} + \frac{1}{2}\sum_{i=1}^{N}(f^{(i)})^2\right] . \tag{8}$$

Where A (i) is a symmetric coefficient matrix, which is the square of vector $\vec{a}$:

$$A^{(i)} = \begin{bmatrix} (a_1^{(i)})^2 & a_1^{(i)}a_2^{(i)} & a_1^{(i)}a_3^{(i)} & \cdots & a_1^{(i)}a_6^{(i)} \\ a_1^{(i)}a_2^{(i)} & (a_2^{(i)})^2 & a_2^{(i)}a_3^{(i)} & \cdots & a_2^{(i)}a_6^{(i)} \\ a_1^{(i)}a_3^{(i)} & a_2^{(i)}a_3^{(i)} & (a_3^{(i)})^2 & \cdots & a_3^{(i)}a_6^{(i)} \\ \vdots & \vdots & \vdots & \ddots & \vdots \\ a_1^{(i)}a_6^{(i)} & a_2^{(i)}a_6^{(i)} & a_3^{(i)}a_6^{(i)} & \cdots & (a_6^{(i)})^2 \end{bmatrix} . \tag{9}$$

We set the ROI as a 7*7 window to reduce the variance of the estimate error. The (8) is equivalent to solve a system equation of

$$A\vec{x} + \vec{b} = 0 . \tag{10}$$

For the 6x6 matrix A of (10) the solution $\vec{x}$ can be obtained from the singular value decomposition [8] SVD of A, we have another form of (10):

$$USV^T\vec{x} + \vec{b} = 0 . \tag{11}$$

Where U and V are orthogonal with the column vectors $\{u_i\}$ and $\{\nu_i\}$, and $S = \mathrm{diag}(\sigma_1, \sigma_2, \ldots, \sigma_n)$ where $\sigma_1 \ge \sigma_2 \ge \ldots \ge \sigma_n \ge 0$ are the singular values of A. Then,

$$\vec{x}_* = \sum_{i=1}^{6} \frac{-\vec{u}_i^T \vec{b}}{\sigma_i}\vec{\nu}_i . \tag{12}$$

IV. Least Squares Formulation with The Regularization

In (10), the matrix A may be ill-conditioned, the eigenvalue of A is small, so σ_i the diagonal elements of the matrix S in (12) are minimum to zero. In that case, the vector calculated by (12) will fail the truth. We extend the LSF with the regularization [9] to overcome the problem. The regularized solution of (11) can be written as:

$$\min_{\vec{x}} E(\vec{x},\alpha) = \min_{\vec{x}}\left[\left\|A\vec{x}+\vec{b}\right\|_2^2 + \alpha\left\|L\vec{x}\right\|_2^2\right] \tag{13}$$

Where $\alpha > 0$ is a constant and L is the regularization matrix, $L \in R^{(N-1)\times N}$ is given by

$$L = \begin{bmatrix} 1 & -1 & & & 0 \\ & 1 & -1 & & \\ & & \ddots & \ddots & \\ 0 & & & 1 & -1 \end{bmatrix}. \tag{14}$$

The minimization (13) is equivalent to the solution of the normal equation,

$$(A^T A + \alpha L^T L)\vec{x} + A^T\vec{b} = 0. \tag{15}$$

In the case of L = I the solution of (15) can be written in terms of the SVD of A as

$$\vec{x}_* = \sum_{i=1}^{n} \frac{-\vec{u}_i^{\,T}\vec{b}}{\sigma_i + \alpha/\sigma_i}\vec{v}_i. \tag{16}$$

It is interesting that if the singular value σ_i is much smaller than α the corresponding term in (16) approaches zero. This demonstrates the required continuity in the solution of a real physical system.

As we use (14) for L, the matrix $L^T L$ is a 6*6 positive definite matrix, and the solution of (15) is not easy to be obtained for different values of α, and cannot be affected using merely the SVD of A as in (16). To save the computational time in the case of using (14) for L, we will solve (15) and $L^T L$ directly, i.e. find the SVD of $A^T A + \alpha L^T L$ and use (12) where $\vec{b} = A^T\vec{b}$.

The basic feature of the regularization is to impose a weak smoothness constraint on the possible solutions. If the matrix L in (15) is the identity, the condition number of the matrix $A^T A + \alpha I$ is given by:

$$\kappa(A^T A + \alpha I) = \frac{\sigma_{max}^2 + \alpha}{\sigma_{min}^2 + \alpha}. \tag{17}$$

Where σ_{max} and σ_{min} are singular values of matrix $A^T A$. Thus the condition number of the regularized matrix $A^T A + \alpha I$ can be much lower than that of the matrix $A^T A$, e.g. for σ_{max}=1, σ_{min}=0.1 and α=0.1 the condition number is improved 10 times (from 100 to 10). Hence, in practical applications, α will always satisfy $\sigma_{min} \le \alpha < \sigma_{max}$. Here we choose σ_{min} as the value of α.

V. Experimental Results

To verify our LSF algorithms we have three groups of controlled trials. The previous two trials compare the simulation image with its original image. The third trial compares the continuous frames of the ultrasound imaging in a real cardiac diagnosis. All images in the experiments used is 200*200 pixels scale. First we calculate the OF of Fig.1(a) with its simulation image Fig.1(b) and Fig. 1(c) to verify the accurate of this algorithm, we compare the calculated velocity strength and direction with the standard strength and direction. The error rate is defined as (18) and (19).

$$e_{length}(x) = \frac{1}{n}\sum_{i=1}^{n}\frac{x-L}{L}. \tag{18}$$

$$e_{direction}(x) = \frac{1}{n}\sum_{i=1}^{n}(x-D). \tag{19}$$

In (18), the X is the velocity of the sampling point, n is the number of the sampling point; L is the standard velocity length. In (19), the X is the angle of the velocity, D is the standard angle. The output vector fields look same as Fig.2(a). The velocity average error rate is 7.27%; the average angle offset is -0.0172 rad. The last experiment, we compare Fig.1(d), the real adjacent frame of Fig.1(a), we get the vector field like Fig.2(c). And we can catch the expansion edge profile of cardiac muscle.

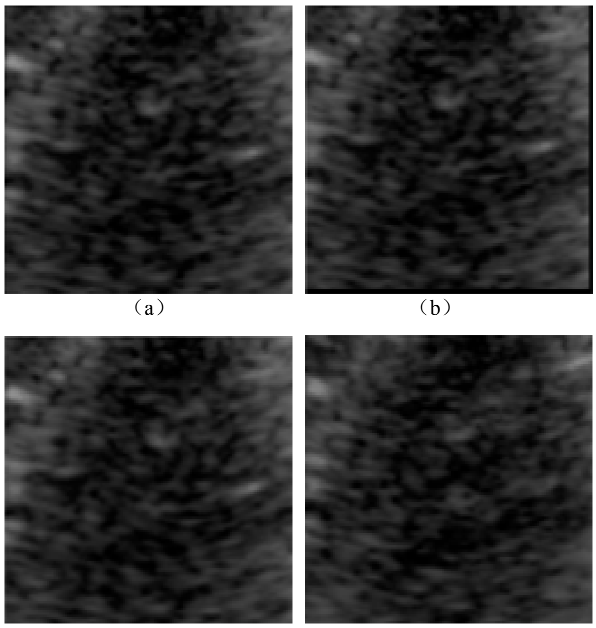

Figure 1. (a)The first frame of the cardiac ultrasound imaging; (b) First frame moves two pixel at both x and y axis direction; (c)First frame make some local distortion; (d) The second frame of the cardiac ultrasound imaging.

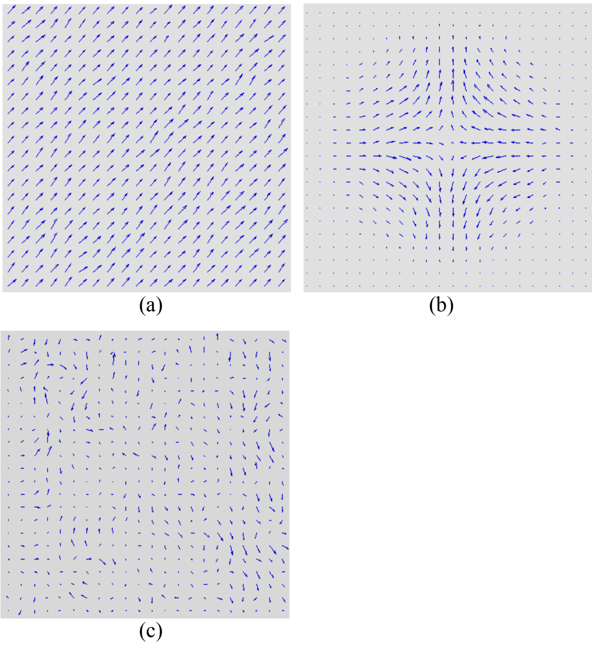

Figure 2. (a)The OF vector diagram of figure 1a and 1b; (b)The OF vector diagram of figure 1a and 1c; (c)The OF vector diagram of figure 1a and 1d

VI. Conclusion And Future Work

In this paper, we present a method to OF computation and successfully apply this algorithm in the motion estimation of cardiac ultrasound imaging. Through the experiment, the result shows this method can accurately get the OF vector field. It has great value in clinical field. However the operation time still can't meet the requirement of the actual ultrasound diagnosis. To our glad, the parallel algorithm has become mature. In the future, we can save much time wasted in matrix operation by transplanting this algorithm to CUDA system [10].

References

[1]. Hom B K． Schunck B G Determining Optical How[J]． Artifical Intelligence, 1981, 17(1—3)：185—204.

[2]. G.H. Golub and C.F. Van Loan, Matrix Computations, The Johns Hopkins University Press, 1983.

[3]. M. J. Black, Robust Incremental Optical Flow, Ph.D. thesis, Yale Univ., New Haven, CT, 1992; Research Report YALEU/DCS/ RR-923

[4]. Baker and I. Matthews, “Lucas-kanade 20 years on: A unifying framework,” International Journal of Computer Vision, vol. 56, no. 3, pp. 221–255, February-March 2004.

[5]. A. Bruhn, J. Weickert, and C. Schn¨orr, “Lucas/Kanade meets Horn/Schunck: combining local and global optical flow methods,” International Journal of Computer Vision, vol. 61, no. 3, pp. 211–231, 2005.

[6] .M. Bertrand, J. Meunier, M. Doucet and G. Ferland, “Ultrasonic biomechanical strain gauge based on speckle tracking”, Proc. Ultrasonics Symp. IEEE, vol.2, 859-863, 1989.

[7]S. Baker, D. Scharstein, J. Lewis, S. Roth, M. J. Black, and R. Szeliski, “A database and evaluation methodology for optical flow,” in Proceedings of the Eleventh IEEE Conference on Computer Vision, 2007.

[8] Wikipedia, Singular Value decomposition, Retrieved Sep.2010. form phttp://en.wikipedia.org/wiki/Singular_value_decomposition

[9]. A.N. Tikhonov, “Solution of incorrectly formulated problems and the regularization method”, Soviet Nath. Dokl., 4, 1035-1038, 1963.

[10]. Lindholm, E., Nickolls, J., Oberman, S., Montrym, J. 2008. NVIDIA Tesla: A unified graphics and computing architecture. IEEE Micro 28(2).